Alaska Terrestrial and Marine Climate Trends, 1957–2021

THOMAS J. BALLINGER,[a] UMA S. BHATT,[b,c] PETER A. BIENIEK,[a] BRIAN BRETTSCHNEIDER,[d] RICK T. LADER,[a] JEREMY S. LITTELL,[e] RICHARD L. THOMAN,[a] CHRISTINE F. WAIGL,[a] JOHN E. WALSH,[a] AND MELINDA A. WEBSTER[c,f]

[a] *International Arctic Research Center, University of Alaska Fairbanks, Fairbanks, Alaska*
[b] *Department of Atmospheric Sciences, University of Alaska Fairbanks, Fairbanks, Alaska*
[c] *Geophysical Institute, University of Alaska Fairbanks, Fairbanks, Alaska*
[d] *NOAA/National Weather Service, Anchorage, Alaska*
[e] *U.S. Geological Survey, Alaska Climate Adaptation Science Center, Anchorage, Alaska*
[f] *Polar Science Center, Applied Physics Laboratory, University of Washington, Seattle, Washington*

(Manuscript received 10 June 2022, in final form 8 February 2023, accepted 4 March 2023)

ABSTRACT: Some of the largest climatic changes in the Arctic have been observed in Alaska and the surrounding marginal seas. Near-surface air temperature (T2m), precipitation (*P*), snowfall, and sea ice changes have been previously documented, often in disparate studies. Here, we provide an updated, long-term trend analysis (1957–2021; $n = 65$ years) of such parameters in ERA5, NOAA U.S. Climate Gridded Dataset (NClimGrid), NOAA National Centers for Environmental Information (NCEI) Alaska climate division, and composite sea ice products preceding the upcoming Fifth National Climate Assessment (NCA5) and other near-future climate reports. In the past half century, annual T2m has broadly increased across Alaska, and during winter, spring, and autumn on the North Slope and North Panhandle (T2m > 0.50°C decade^{-1}). Precipitation has also increased across climate divisions and appears strongly interrelated with temperature–sea ice feedbacks on the North Slope, specifically with increased (decreased) open water (sea ice extent). Snowfall equivalent (SFE) has decreased in autumn and spring, perhaps aligned with a regime transition of snow to rain, while winter SFE has broadly increased across the state. Sea ice decline and melt-season lengthening also have a pronounced signal around Alaska, with the largest trends in these parameters found in the Beaufort Sea. Alaska's climatic changes are also placed in context against regional and contiguous U.S. air temperature trends and show ~50% greater warming in Alaska relative to the lower-48 states. Alaska T2m increases also exceed those of any contiguous U.S. subregion, positioning Alaska at the forefront of U.S. climate warming.

SIGNIFICANCE STATEMENT: This study produces an updated, long-term trend analysis (1957–2021) of key Alaska climate parameters, including air temperature, precipitation (including snowfall equivalent), and sea ice, to inform upcoming climate assessment reports, including the Fifth National Climate Assessment (NCA5) scheduled for publication in 2023. Key findings include widespread annual and seasonal warming with increased precipitation across much of the state. Winter snowfall has broadly increased, but spring and autumn snowfalls have decreased as rainfall increased. Autumn warming and precipitation increases over the North Slope, in particular, appear related to decreased sea ice coverage in the Beaufort Sea and Chukchi Seas. These trends may result from interrelated processes that accelerate Alaska climate changes relative to those of the contiguous United States.

KEYWORDS: Arctic; Sea ice; Climate; Precipitation; Snowfall; Temperature

1. Introduction

The rapid rate of recent environmental changes in Alaska warrants revisiting climate trends while assessing the current state of Alaska's physical system in the process (Thoman and Walsh 2019). The physiographic variation in Alaska is substantial, such that the variation in these trends and the impacts they are causing should be evaluated at subregional scales when possible; the perhumid southeast Alaska coast experiences many climate changes differently than the Arctic North Slope, but other changes are held in common across the state.

While no single study can capture all the relevant trends and their details, our analyses herein attempt to characterize trends that underlie many of the serious impacts affecting the land and seascapes, habitats, species, and people in the state, and for which the most robust datasets exist. Such trends, including those of surface air temperature, precipitation, and snowfall specifically, as well as sea ice, support decision-making and provide partial foundational information for adaptation planning and vulnerability assessments (e.g., Mizukami et al. 2022). Quantifying changes in these parameters through time does not substitute for near-term, multiyear forecasts. However, despite uncertainties enmeshed in chaotic climate variability, the rates

Denotes content that is immediately available upon publication as open access.

Supplemental information related to this paper is available at the Journals Online website: https://doi.org/10.1175/JCLI-D-22-0434.s1.

Corresponding author: Thomas J. Ballinger, tjballinger@alaska.edu

DOI: 10.1175/JCLI-D-22-0434.1

of such changes are important indicators of plausible near-future trends as well.

The goal of our present study is to produce an updated analysis of trends in the physical drivers of climate impacts in Alaska. The study is motivated by the need to provide robust assessments of rates of change that, in turn, provide a foundation in forthcoming impacts and risk statements, such as the upcoming Fifth National Climate Assessment (NCA5) narrative. Doing so requires attention to both terrestrial and marine parameters and their means and extremes. Specifically, we update and analyze long-term trends in near-surface air temperature, precipitation, snowfall water equivalent, and sea ice extent along with melt/freeze onset, which may serve as a reference for future climate reports.

Our paper follows with a review of Alaska climate research in section 2. An overview of the study area is presented in section 3. Data and methods are described in section 4. Results are presented in section 5, and section 6 provides discussion and context to relevant findings. A brief summary and conclusions are offered in section 7.

2. Review of Alaska climate variations and trends

Information on variations and trends of Alaska's climate has appeared in broader climate assessments as well as studies specific to Alaska. Most of the earlier studies were based on station data records or aggregations of station data. As far back as the IPCC's Third Assessment report in 2001, Alaska's temperature variations were shown to be part of a broader pattern of Arctic amplification characterized by multidecadal variations (IPCC 2001, their Fig. 3). A temporal pattern of early twentieth century warming, mid-twentieth century cooling, and late twentieth century warming has been diagnosed in terms of internal variability, natural forcing (primarily aerosols), and anthropogenic forcing by Fyfe et al. (2013). The Arctic Climate Impact Assessment showed that the late twentieth century (1966–2003) warming over Alaska spanned all seasons (Arctic Monitoring and Assessment Programme 2005, their Fig. 2.8). A large component of the internal variability has been shown to be attributable to the Pacific decadal oscillation (PDO) (Hartmann and Wendler 2005). López-de-Lacalle (2012) extended this work, using long-term records from six Alaska stations, to show that the phase of the PDO leads to excursions of up to 4°C in seasonal air temperature, with the strongest impacts of the PDO occurring in winter. However, López-de-Lacalle et al. (2012) also showed that an overall increase in temperature is superimposed on the excursions associated with the PDO. This finding was confirmed by Bieniek et al. (2014) using records of Alaska climate divisional temperatures extending back to 1920. More recently, Walsh and Brettschneider (2019) diagnosed Alaska's temperature trends over the 1950–2017 period, showing that the warming exceeds that attributable to the atmospheric circulation-driven component by 2.1°C in winter and spring, 1.3°C in summer, and 0.5 °C in autumn. These findings are consistent with the trends simulated by global climate models run with historical and projected greenhouse gas concentrations for the same period. The warming of Alaska has continued into the recent decade based on syntheses of station-based analyses (Vose et al. 2017; Markon et al. 2018). Bigalke and Walsh (2022) analyzed ERA5 air temperature data and showed that the Alaska warming through 2020 is part of the broader Arctic warming during the winter season (December–February); however, their study did not evaluate ERA5 trends annually or for other seasons.

In contrast to the warming signal in Alaska's temperatures over the past several decades, there is little evidence for significant trends in precipitation or extreme precipitation events over Alaska (Bieniek and Walsh 2017; Lader et al. 2017; Bachand and Walsh 2022). However, data limitations confound the evaluation of precipitation trends because (i) precipitation gauges are known to suffer from the undercatchment of snowfall in cold, windy environments (Yang et al. 2005); (ii) the station network in Alaska is sparse and biased toward low elevations and coastal regions; and (iii) Alaska's topography introduces large spatial gradients into precipitation amounts in winter, and the spatial heterogeneity is compounded by the convective nature of warm-season precipitation. Heterogeneities in station records have been documented by McAfee et al. (2013), while gridded products have also been shown to contain inconsistencies (McAfee et al. 2014). The latter inconsistencies affect the magnitude and even the sign of computed trends of precipitation (McAfee et al. 2014).

In view of the uncertainties inherent in station-based datasets, atmospheric reanalyses offer a potentially attractive alternative to evaluations of variations in precipitation over Alaska. However, the model dependence of reanalysis output calls for another layer of evaluation. White et al. (2021) used Bayesian statistical methods in an attempt to distinguish discontinuities and trends in precipitation over Alaska. This approach identified spurious discontinuities in several station records for southeast Alaska, associated with the change to automated observations in the early 1990s. Discontinuities did not appear in ERA5 when satellite data assimilation increased in 1979. The results also pointed to a general absence of a strong signal of precipitation change over Alaska, consistent with previous studies. However, there were two exceptions: 1) an increase of precipitation over Alaska's North Slope and 2) indications of a broader emerging signal (positive trends) when the most recent decade was included. The ERA5 reanalysis used by White et al. (2021) has been shown to provide a more accurate depiction of Arctic precipitation relative to the earlier NCEP–NCAR and ERA-Interim reanalyses (Wang et al. 2019; Cabaj et al. 2020). McCrystall et al. (2021) also evaluated ERA5 output over the Arctic Ocean and found that it showed better agreement with climate model simulations than did the merged satellite and gauge-based product of the Global Precipitation Climatology Product (McCrystall et al. 2021, their Fig. 1).

Offshore, reductions in annual and summer sea ice have been documented in the adjacent Beaufort and Chukchi Seas during 1979–2012 (Frey et al. 2015), while anomalously low winter ice extents in the Bering Sea have occurred most years within the last decade (Ballinger and Overland 2022). Of particular relevance to surface air temperatures is the lengthening of the open-water season along the northern and western Alaska coasts (Rolph et al. 2018). Evidence of an association between reduced sea ice cover, higher air temperatures, and increased vegetative greenness has been presented by Bhatt et al. (2021).

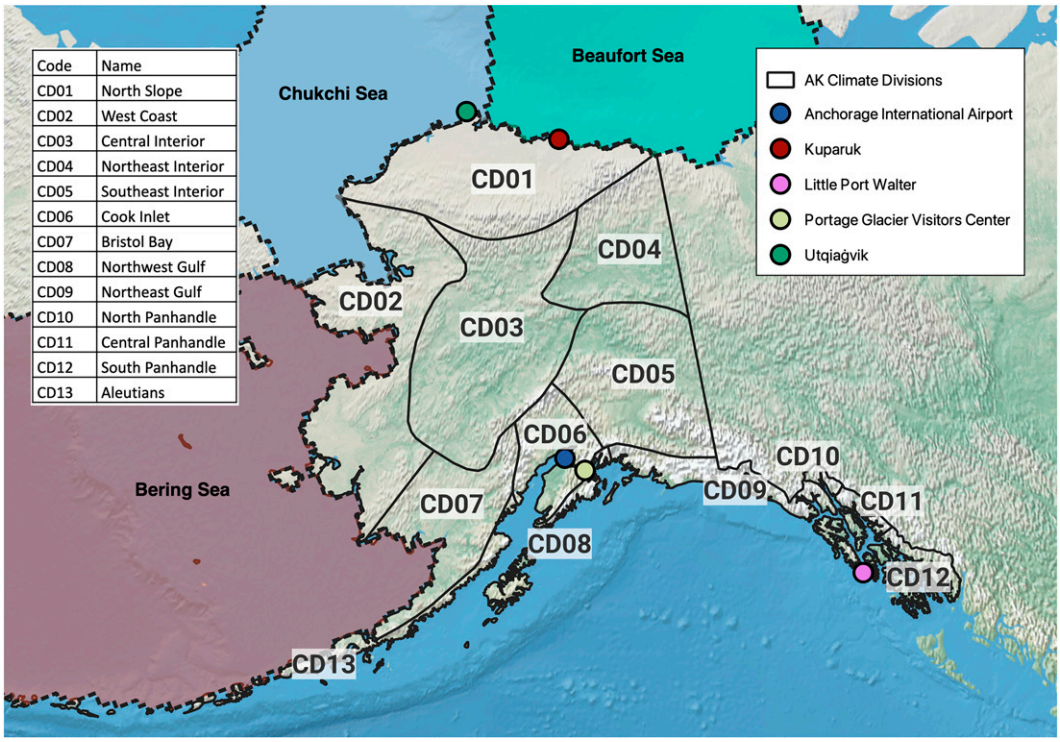

FIG. 1. Map showing the 13 Alaska climate divisions, and the masked sea ice regions, Bering Sea, Beaufort Sea, and Chukchi Sea, analyzed in this study. Locations mentioned in the manuscript are also marked for reference. The base map is from Natural Earth (https://www.naturalearthdata.com/; Earth Resources Observation and Science Center/U.S. Geological Survey/U.S. Department of the Interior 1997; Farr et al. 2007).

The increase of air temperatures during the nonsummer seasons has also been implicated in the shortening of the snow season over Alaska statewide (Thoman and Walsh 2019, p. 7), although the latter result was based on only about 20 years of data. Another limited-duration (16-yr) study of the snow cover in Alaska's Arctic national parks showed a shorter duration of snow cover by six days (Swanson 2017). One of the goals of the present paper is to provide a more comprehensive assessment of changes in Alaska's sea ice and snow.

3. Study areas

As the largest state in the United States, Alaska spans a wide range of latitude and biomes, from the Arctic (Alaska's North Slope) to the temperate rain forests of the Alaska Panhandle extending southward to about 54°N. The wide range of climate conditions is captured by a classification of Alaska's land area into 13 climate divisions developed by Bieniek et al. (2012; Fig. 1) that have been used operationally by the National Oceanic and Atmospheric Administration's National Centers for Environmental Information (NOAA NCEI) since 2015. While most of these divisions are larger than those in the contiguous United States (one notable exception is the North Panhandle), they were developed by Bieniek et al. (2012) on the basis of the spatial coherence of variations in temperature and precipitation measurements at observing stations. It should be noted that Alaska's network of historical first-order observing stations is sparse when compared to other parts of the United States. The stations are unevenly distributed and tend to be located proximate to population centers and research sites, with more both in the south than in the north and near the coast than inland, and all at low (i.e., valley level) elevations. The low elevations are characteristic of the inland stations as well as those along the coast.

Alaska is surrounded by seas to its north, west, and south. The Beaufort and Chukchi Seas to the north are covered by sea ice for much of the year, while a seasonal ice cover of several months' duration characterizes much of the Bering Sea west of Alaska. The cold climate of Alaska results in an extensive snow cover that persists for 6–7 months over much of southern Alaska and 8–10 months over the Interior and North Slope (Lindsay et al. 2015). The timing of the retreat of sea ice and terrestrial snow cover is largely atmospherically driven, and these associations are apparent in interannual variability as well as trends over time.

Alaska's main topographic features are the coastal mountains, the Alaska Range extending in an arc across south-central Alaska, and the Brooks Range, which separates the North Slope from the state's interior. The coastal mountains and the Alaska Range contain considerable glacierized area, with ice fields, alpine glaciers, and tidewater glaciers that terminate in the Gulf of Alaska. Approximately two-thirds of Alaska is underlain by permafrost, ranging from isolated patches in the southern regions to deep continuous permafrost on the North Slope poleward of the Brooks Range.

4. Data and methods

a. Spatiotemporal scales

Terrestrial 2-m air temperature (T2m); precipitation (P), defined as the sum of rain plus water equivalent of frozen precipitation (e.g., melted snow); and snowfall water equivalent (SFE) statistics, as described in section 4b, are calculated for the 13 standard Alaska climate divisions shown in Fig. 1. Climate division names and codes are used interchangeably as shown and defined in the figure. The sea ice region masks of Meier et al. (2022) are used in calculating Bering Sea, Beaufort Sea, and Chukchi Sea ice cover statistics. The sea ice regions are also shown in Fig. 1.

We constrain analyses to the beginning of the International Geophysical Year (IGY; 1957), which marked the time when global radiosondes measurements were standardized to 0000 and 1200 UTC (Grant et al. 2009). Consistency of the radiosonde network is especially important for atmospheric reanalyses that assimilate available observations; as described in section 4b, atmospheric reanalysis products are key sources of information in the present study. In addition, there was a general increase in the number of Arctic weather observations during the IGY period (Walsh et al. 2018). Some potentially erroneous surface air temperature values in the Bering Sea region pre-IGY (e.g., St. Lawrence Island during summers 1950–52; Fig. S1 in the online supplemental material) further supports the choice of the IGY period as a starting point for a consistent historical analysis. The one exception is satellite-derived melt/freeze onset data, which are constrained to 1979–2021. Given the sensitivity of trends to the starting and ending dates, we address the dependence on starting date in section 5.

b. Data

For terrestrial analyses, daily T2m (°C), P (cm or mm), and SFE (mm) for Alaska are obtained from ERA5 global reanalysis at 31-km spatial and hourly temporal resolution, for 1957–2021 (Hersbach et al. 2020). ERA5 SFE represents the sum of large-scale and convective snowfall, in mm water equivalent. Unless otherwise indicated, grid cells within each climate division are averaged prior to statistics being calculated. ERA5 offers numerous improvements relative to its predecessor, ERA-Interim, including but not limited to the model cycle (Cy41r2 vs Cy31r2), horizontal [31 km (TL639) vs 79 km (TL255)] and vertical resolution (137 vs 60 levels), and time stepping (hourly analysis fields vs 6-hourly). ERA5 is also characterized by an increase in data volume with time, especially from satellite radiances, and recent developments in terrestrial, oceanic, and atmospheric data assimilation methods; such improvements and an overview of newly added data are chronicled in detail in Hersbach et al. (2020).

The ERA5 reanalysis has been used in recent interannual Arctic climate assessments (Moon et al. 2021) and has been shown to compare well against observations over Arctic land and marine areas with reduced air temperature biases relative to other modern atmospheric reanalyses (Graham et al. 2019; Avila-Diaz et al. 2021). ERA5 has also been shown to be effective in capturing boreal high-latitude trends of T2m and P, including rainfall and snowfall (Barrett et al. 2020; Räisänen 2021; Dou et al. 2021; McCrystall et al. 2021). However, ERA5 SFE trends should be interpreted with caution at high elevations, as accumulated snow tends to be overestimated above 1500 m (Hersbach et al. 2020). More specific to Alaska analyses herein, recent studies have shown that ERA5 is also robust against observations and, therefore, represents a valid gridded product for the assessment of statewide precipitation trends (White et al. 2021) and extremes (Bachand and Walsh 2022). It should be noted that ERA5 does not assimilate precipitation data over Alaska (H. Hersbach, ECMWF, 2022, personal communication).

ERA5's hourly analysis fields, periodically supplemented with short-range forecasts (Hersbach et al. 2020), provide an improved depiction of regional climate variables over, for example, those derived from the 5-km NOAA monthly climate gridded dataset (NClimGrid) derived from Global Historical Climatology Network daily data (Vose et al. 2014). This point is illustrated in Fig. 2, where 65-yr annual trends derived from

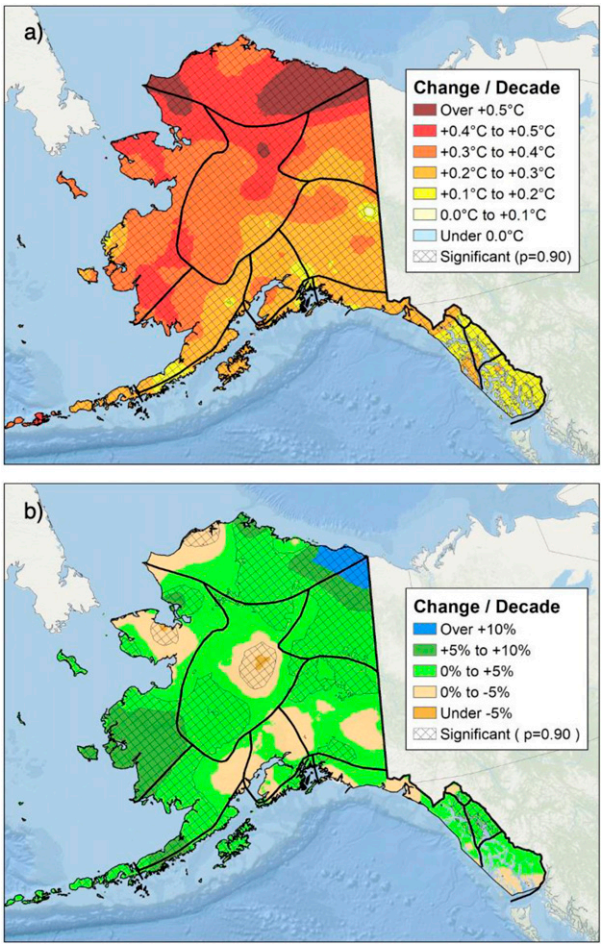

FIG. 2. NOAA NClimGrid 4-km gridded annual Theil–Sen trends, 1957–2021, for (a) T2m (°C decade^{-1}) and (b) precipitation (% decade^{-1}). Significant trends, where $p \leq 0.10$, are hatched.

TABLE 1. Annual Alaska statewide T2m OLS and Theil–Sen trends (°C decade^{-1}) based on NCEI ACD data described by Vose et al. (2017).

Period	OLS trend (°C decade^{-1})	Theil–Sen trend (°C decade^{-1})
1957–2021	0.34	0.35
1951–2021	0.35	0.34
1961–2021	0.40	0.43
1971–2021	0.45	0.50
1981–2021	0.37	0.43
1991–2021	0.44	0.53

NClimGrid show unrealistic patterns evidenced as "bullseyes" in the trends and significance fields. These patterns result from data quality and procedural issues that degrade the division-wide T2m and *P* monthly series when examined over multidecade time scales. A multitude of factors contribute to these issues, including very low data density (especially in northern and western Alaska), low elevation bias, missing and incorrect data values, variable reporting intervals, station relocation, and period of record. While the problems are most obvious for *P* trends (Fig. 2b), station-based artifacts are also readily identifiable in the T2m trend (Fig. 2a). Additional comparisons between ERA5 and the NOAA NCEI Alaska climate division (hereafter abbreviated as NCEI ACD) T2m and *P* time series are also discussed in section 4c(3). The weather station data and statistical methods used to construct these NCEI datasets are described in Bieniek et al. (2014) and Vose et al. (2017).

With regard to trends of precipitation, we note here that the use of ERA5 for precipitation variables offers a framework of consistent precipitation-product generation, subject to the constraint that the assimilated observational data can change over time. Alternative gridded precipitation products (e.g., the Global Precipitation Climatology reanalysis, the University of Delaware precipitation product, the U.K. Climate Research Unit's precipitation database) have been shown to contain heterogeneities that largely preclude their use in trend analyses for Alaska (McAfee et al. 2014).

Sea ice extent (SIE) data for the Alaska region from 1957 to 1978 is based on the historical sea ice atlas of Walsh et al. (2017; see also https://www.snap.uaf.edu/tools/sea-ice-atlas) and the monthly National Snow and Ice Data Center (NSIDC) Sea Ice Index, version 3, for Arctic regions (Fetterer et al. 2017) from 1979 to 2021. The earlier and later time series were homogenized by adjusting the sea ice atlas by the offsets of the March and September monthly means for the overlap period of 1979–90. The bias adjustments of the earlier data were calculated separately for the Chukchi, Beaufort, and Bering Seas. The resulting SIE time series are shown for September in the Chukchi Sea and Beaufort Sea and March in the Bering Sea, which represent the respective months of climatological minimum and maximum SIE. Sea ice melt and freeze onset dates, derived from passive microwave brightness temperatures (Markus et al. 2009), were also used to evaluate the long-term changes in melt onset, freeze onset, and melt-season duration in these three marginal seas.

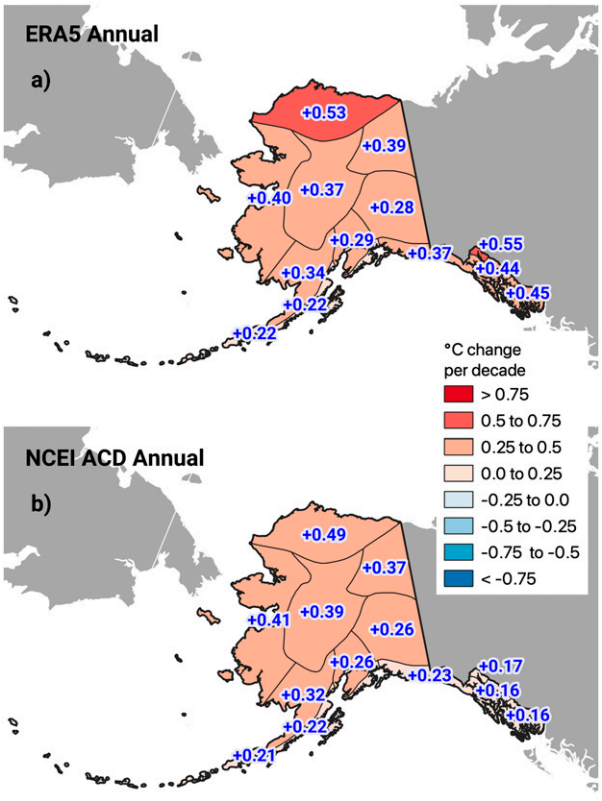

FIG. 3. Annual T2m Theil–Sen climate division trends (°C decade^{-1}) for (a) ERA5 and (b) NCEI ACD. All values shown are statistically significant at $p \leq 0.10$.

c. *Methods*

1) MEAN AND EXTREME CALCULATIONS

ERA5 hourly data (Hersbach et al. 2020) for the full time period, 1957–2021, are aggregated to standard seasonal means (DJF, MAM, JJA, and SON) and annual (i.e., January–December) averages for T2m, precipitation, and SFE. For analyses of T2m and *P* extremes, the ERA5 data are averaged to a daily time step and used to calculate climatological mean values of the 1st (T01) and 99th percentiles (T99) of T2m, and maximum 1-day (RX1) and 5-day (RX5) *P* amounts. The consideration of other seasonal definitions and the associated sensitivity of results to these definitions (i.e., snow and sea ice) are described in the context of the data and methods. Trends of the annual time series for each index were computed using methods described in the following section.

2) HOMOGENEITY TESTING

Unlike *P*, T2m from Alaska surface weather stations is assimilated into ERA5 (H. Hersbach, ECMWF, 2022, personal communication). We applied the Pettitt changepoint technique

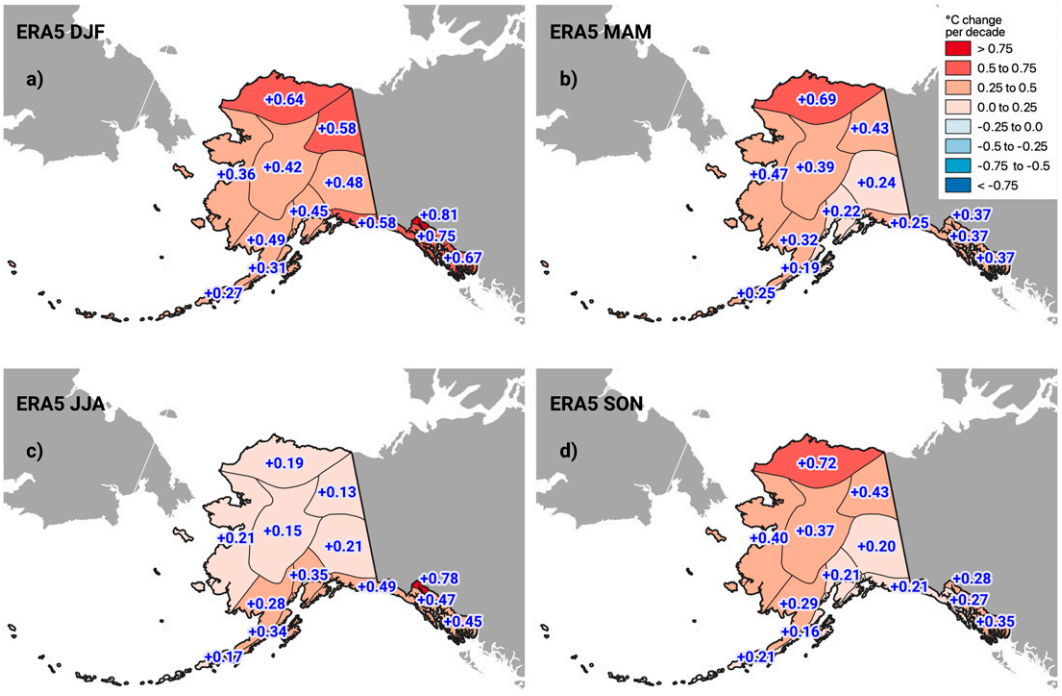

FIG. 4. Seasonal ERA5 T2m Theil–Sen climate division trends (°C decade^{-1}), 1957–2021, for (a) winter (DJF), (b) spring (MAM), (c) summer (JJA), and (d) autumn (SON). All values shown are statistically significant ($p \leq 0.10$).

(Pettitt 1979) to assess whether potential inhomogeneities in T2m arise through time as a result of the number of assimilated weather stations and/or total observations from those stations. This approach is designed to isolate mean or variance changes between two segments within a time series. We find that breaks in the ERA5 climate division T2m (Fig. S2) generally do not match analogous temporal changes in total station observations or singular weather station counts from mainland or southeast Alaska that are assimilated into ERA5 (Fig. S3). It should be noted that the identification of climate division temporal changes is generally consistent between different changepoint techniques (e.g., Buishand range test, standard normal homogeneity test; results not shown). As we might expect, T2m changes over some Alaska climate divisions (e.g., Northeast Gulf, Northwest Gulf, North Panhandle) are aligned with the documented PDO shift in 1976 (Hartmann and Wendler 2005).

3) TREND ESTIMATION AND COMPARISONS

Seasonal and annual precipitation trends over 1957–2021 from ERA5, and additionally the NCEI ACD data where appropriate, were analyzed by three different methods: ordinary least squares regression (OLS), Theil–Sen regression (Theil 1950; Sen 1968) and gamma regression (generalized linear model with a specified gamma distribution; e.g., Nelder and Wedderburn 1972). The P and SFE trends are much more heterogeneous than T2m trends, and their results differ depending on the datasets and analysis techniques used. This is due, in part, to spatial variability of precipitation, modeling of precipitation (i.e., in ERA5), variable availability, and the reliability of extremely sparse in situ networks in Alaska from which to construct a dense grid.

We aggregated hourly T2m and P data at the divisional level to annual and seasonal means or totals, but for SFE, we considered DJF, MAM, and SON, and additional snow seasons that characterize the range of snow-accumulation seasons in Alaska: September to the following August (ANN), NDJFM, and October–April (ONDJFMA). We did not evaluate JJA SFE because, at the scale of climate divisions, the preponderance of zero values limits estimation. Theil–Sen slope and p estimates were extracted from regressions run using the R package "trend" (Pohlert 2020). Gamma regressions were computed as generalized linear models (glm) with a gamma family distribution and a log link. We considered trends significant if tests met the criteria for the 90% confidence level where p ($|t|$ for OLS and gamma, or $|\tau|$ for Theil–Sen) is $\leq$0.10. In the analyses below, we mainly present Theil–Sen trend estimates and associated Mann–Kendall estimates of p values, but we refer to other tests as necessary.

5. Results

a. Temperature

Our evaluation of trends will focus on the period 1957–2021 for the reasons presented in section 4. However, this choice of the time frame must be accompanied by an acknowledgment that the trends are sensitive to the start date (as well as the end date). To illustrate this sensitivity, Table 1 shows OLS and Theil–Sen trends of the annual statewide Alaska temperature for various start dates, including 1957 as well as other

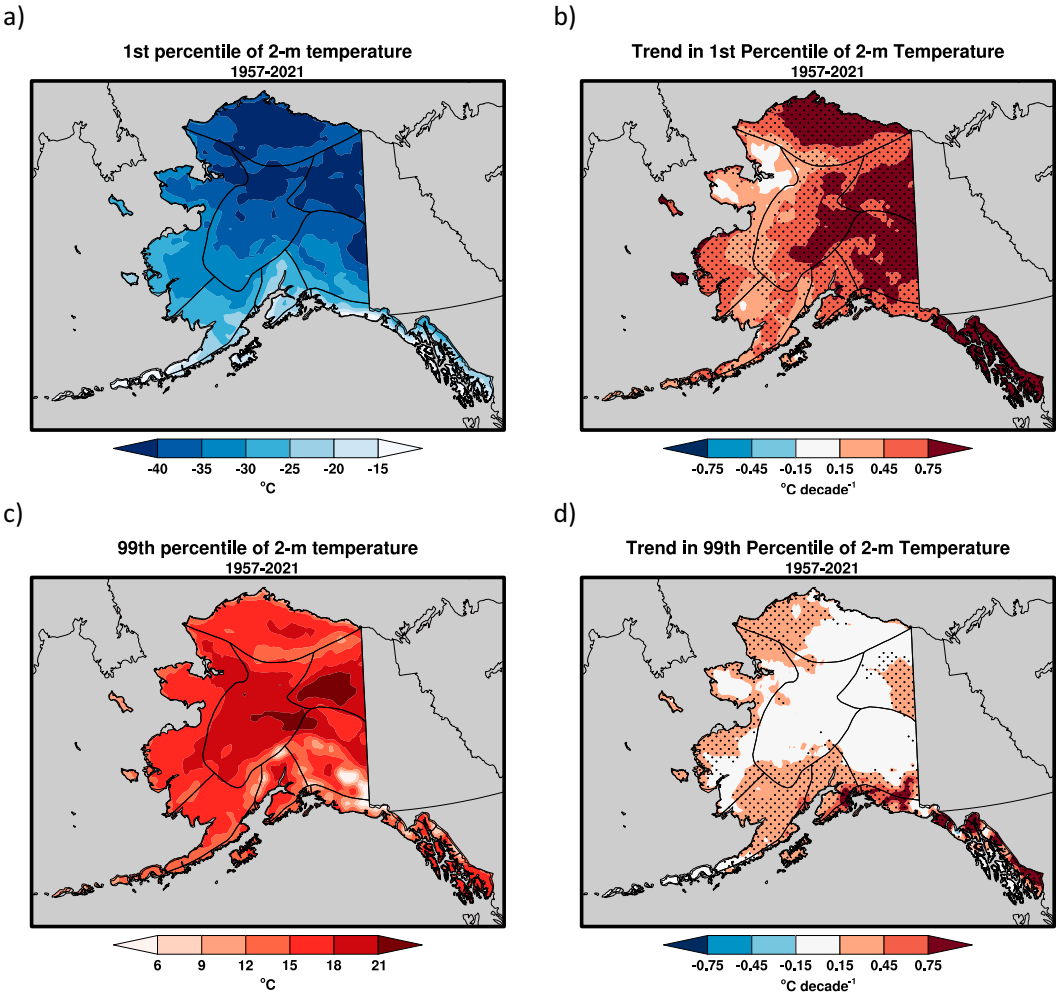

FIG. 5. (left) Mean values (°C) and (right) Theil–Sen trends (°C decade^{-1}) of annual (a),(b) 1st percentile of T2m and (c),(d) 99th percentile of T2m. Significant trends, where $p \leq 0.10$, are stippled.

start-of-decade alternatives. Trend magnitudes tend to be slightly greater in Theil–Sen than OLS, especially for periods starting in or after 1961, which may be due to the aforementioned methodological differences. In general, magnitude differences among time periods arise from internal variations of the annual temperatures; for example, a series of cold years in the 1970s followed by warm years in the early 1980s (associated with a shift in the PDO) account for the weaker trend when the start date shifts from 1971 to 1981. Nevertheless, several conclusions emerge from Table 1. First, despite some internal variability, the general magnitude of the trend does not vary substantially with the choice of start dates. Second, the trend for the 1957–2021 period utilized in this study is at the low end of the range of values. With these conclusions and caveats in mind, we proceed to a more detailed presentation of the temperature trends.

Annually, the ERA5-based T2m trend is positive and statistically significant (i.e., $p \leq 0.10$) for all climate divisions (Fig. 3a). The largest Theil–Sen trends, T2m > 0.50°C decade^{-1}, are observed for the North Slope and North Panhandle divisions. Analogous NCEI ACD (Bieniek et al. 2014) annual T2m trends likewise indicate positive and statistically significant decadal changes across divisions (Fig. 3b). Trend magnitudes are roughly similar between products across interior Alaska, including for the largest trends at the North Slope division. However, there are large deviations in ERA5 versus NCEI ACD trends ($\geq$0.28°C decade^{-1}) at the three panhandle divisions where topographic complexity presents challenges for regional trend estimates.

Similar to the annual ERA5 trends, seasonal trends are positive and statistically significant across all divisions and during all seasons (Fig. 4). The largest trends by season are found either for the North Slope [T2m $\geq$ 0.69°C decade^{-1} in spring and autumn (Figs. 4b,d)] or North Panhandle [T2m $\geq$ 0.78°C decade^{-1} in winter and spring (Figs. 4a,c)]. Winter has the largest trends across divisions, most notably in ERA5 in the divisions flanking the northeastern Gulf of Alaska (T2m $\geq$ 0.58°C decade^{-1} at the Northeast Gulf, North Panhandle, Central Panhandle, and South Panhandle). The North Slope and West Coast divisions during spring and autumn, near regions of early sea ice retreat and

TABLE 2. ERA5 mean values and Theil–Sen trends of annual 1st percentile of T2m temperature (T01) and 99th percentile of T2m temperature (T99) from 1957 to 2021. Significant trends that met the 90% confidence level are in bold.

Climate division	Code	T01 mean (°C)	T01 trend (°C decade^{-1})	T99 mean (°C)	T99 trend (°C decade^{-1})
North Slope	CD01	−39.77	**0.81**	15.28	0.15
West Coast	CD02	−32.94	**0.38**	16.10	**0.18**
Central Interior	CD03	−36.78	**0.66**	18.27	0.10
Northeast Interior	CD04	−40.38	**0.81**	18.60	0.13
Southeast Interior	CD05	−33.94	**0.86**	15.05	**0.15**
Cook Inlet	CD06	−24.02	**0.55**	14.37	**0.34**
Bristol Bay	CD07	−26.29	**0.41**	14.90	**0.22**
Northwest Gulf	CD08	−15.99	**0.36**	13.18	**0.34**
Northeast Gulf	CD09	−18.68	**0.87**	11.50	**0.50**
North Panhandle	CD10	−25.97	**1.32**	12.72	**0.97**
Central Panhandle	CD11	−18.95	**1.26**	13.08	**0.34**
South Panhandle	CD12	−14.31	**1.27**	15.05	**0.41**
Aleutians	CD13	−8.66	**0.34**	11.61	**0.12**

extended periods of open water, respectively, have the largest trends, while summer trends are largest at divisions near the Gulf of Alaska.

Extreme temperatures from ERA5 showed widespread, significant, and increasing trends at both the 1st (T01) and 99th (T99) percentiles, indicating cold and warm extremes, respectively (Fig. 5). To highlight the aforementioned orographic dependence on extremes across the state, spatial plots of extremes are shown and supplemented by climate division–aggregated means and extremes listed in Table 2 and described here. Mean climatological values of T01 ranged from −40.38°C in the Northeast Interior to −8.66°C in the Aleutians. All T01 trends were statistically significant at the 90% confidence level, with the largest trend in South Panhandle (1.27°C decade^{-1}) and the smallest in the Aleutians (0.34°C decade^{-1}). Historical mean values of T99 ranged from 11.50°C in the Northeast Gulf to 18.60°C in the Northeast Interior. All trends of T99 were positive; however, they were only significant across southern and western Alaska mainland divisions, but not in the Central Interior, North Slope, and Northeast Interior divisions.

b. *Precipitation*

Precipitation in Alaska is extraordinarily variable due to the diversity of climates and dramatic impact of complex terrain. For climate stations with NOAA-published, 1991–2020 average annual total precipitation, totals vary from less than 120 mm at Kuparuk (coastal North Slope) to more than 6200 mm at Little Port Walter (Baranof Island) (data available at https://www.ncei.noaa.gov/products/land-based-station/us-climate-normals; for methodology see Arguez et al. 2012). Even within comparatively compact regions, precipitation can vary enormously. For example, within the Municipality of Anchorage, home to ~40% of Alaska's population and near sea level, the average annual total precipitation ranges from near 400 mm (Anchorage International Airport) to more than 4000 mm (Portage Glacier Visitors Center; see Fig. 1).

Annual precipitation trends from ERA5 at the climate division level are much more heterogeneous than temperature (Fig. 6a). Annual total precipitation trends over 1957–2021 are positive in all climate divisions but are significant only for the North Slope (3.22% decade^{-1}) and Southeast Interior (1.16% decade^{-1}). Of note, Bristol Bay and the adjacent Northeast Gulf divisions exhibit trends that are significant in both OLS and gamma regression but not via the Theil–Sen method. Comparatively, while the ERA5 and NCEI ACD data show trends of similar sign across divisions, the NCEI ACD magnitudes are generally larger (Fig. 6b). This difference is

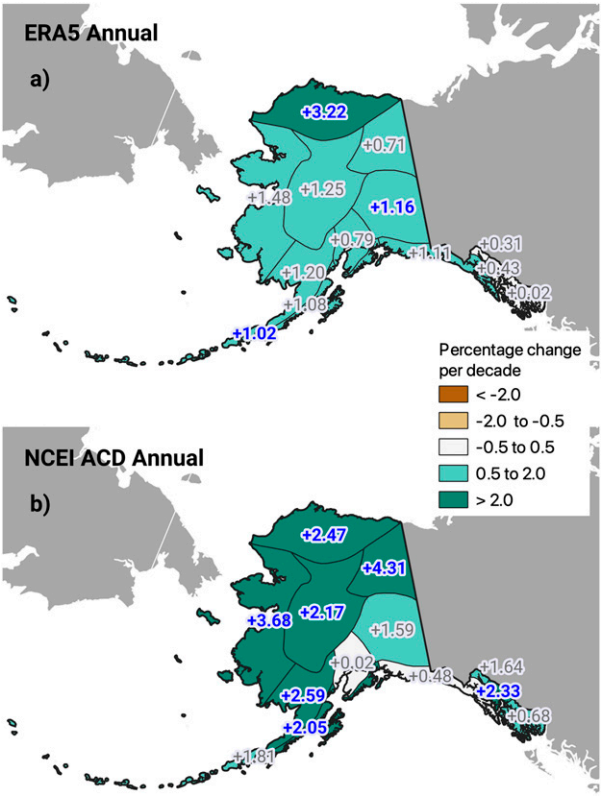

FIG. 6. Annual precipitation Theil–Sen climate division trends (% decade^{-1}) for (a) ERA5 and (b) NCEI ACD. Blue, bolded values indicate trends that are statistically significant at $p \leq 0.10$.

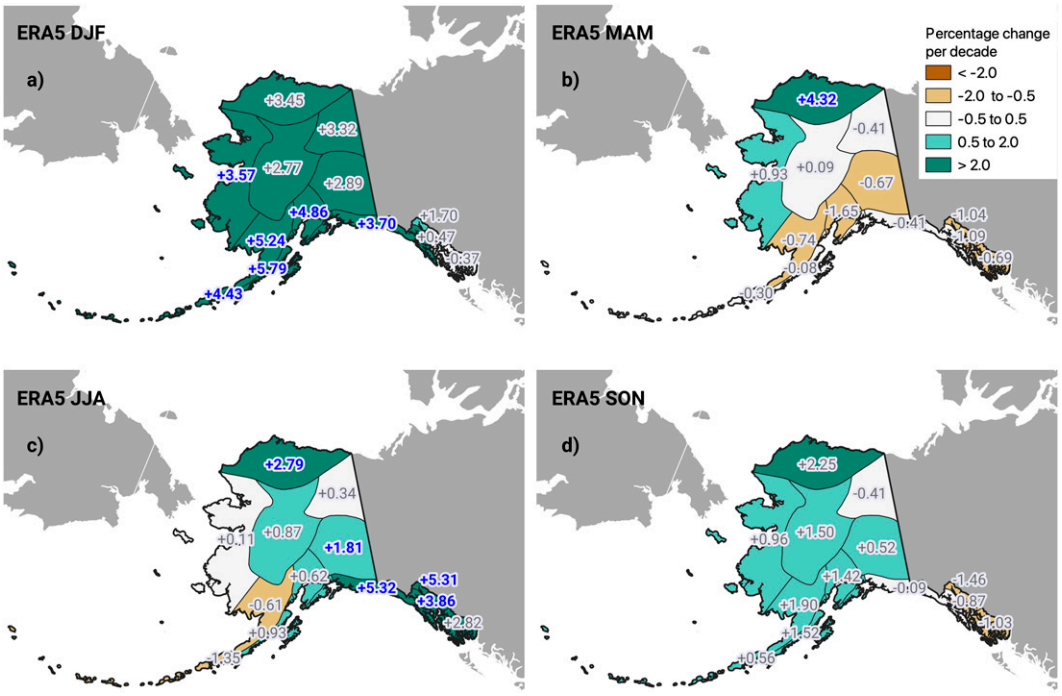

FIG. 7. Seasonal ERA5 precipitation Theil–Sen climate division trends (% decade^{-1}), 1957–2021, for (a) winter (DJF), (b) spring (MAM), (c) summer (JJA), and (d) autumn (SON). Blue, bolded values indicate trends that are statistically significant at $p \leq 0.10$.

especially apparent for the West Coast, Central Interior, Northeast Interior, and the Panhandle climate divisions.

Seasonally, positive trends are most widespread in winter (Fig. 7a) and summer (Fig. 7c), while precipitation in the transition seasons tends to have very little trend (Figs. 7b,d). Trends are significant at the 90% confidence level in six (five) divisions in winter (summer). However, only the Northeast Gulf division has a significant trend in both winter (3.70% decade^{-1}) and summer (5.32% decade^{-1}). Autumn shows no significant trend in any division and spring only in the North Slope division. Although not individually statistically significant, it is notable that in spring, every division except for the North Slope and West Coast has zero or slightly negative precipitation trends. In autumn, the negative trends are mostly confined to the Northeast Gulf coast and three Panhandle divisions.

Trends of RX1 and RX5 precipitation from ERA5 were mixed across Alaska (Fig. 8). At the climate-division scale, mean climatological values of RX1 ranged from 1.73 cm in the North Slope to 7.81 cm in the Northeast Gulf; for RX5, these values ranged from 3.64 cm in the Northeast Interior to 19.36 cm in the Northeast Gulf (Table 3). The only divisions with significant trends at the 90% confidence level were the North Slope and the Southeast Interior. Trends of RX1 and RX5 in the North Slope were 2.34% and 2.17% decade^{-1}, respectively; in the Southeast Interior these were 1.42% and 1.74% decade^{-1}, respectively.

c. *Snowfall*

Across 12 divisions, MAM (mean, −3.4% decade^{-1}), SON (mean, −2.9% decade^{-1}), and annual (September–August: mean, −1.1% decade^{-1}) SFE slopes were negative, but not all were statistically significant. The lone exception was the North Slope, where positive (if not significant) SFE trends were found in all seasons. Meanwhile, a significant trend in annual SFE was only detected in the South Panhandle (−3.29% decade^{-1}; Table 4). However, significantly decreasing spring (MAM) and autumn (SON) trends were evident, primarily but not exclusively in southern Alaska. Spring SFE decreased significantly in the Southeast Interior (−3.32% decade^{-1}), Cook Inlet (−3.72% decade^{-1}), Bristol Bay (−4.95% decade^{-1}), Central Panhandle (−3.13% decade^{-1}), and Aleutians (−4.46% decade^{-1}). For the Central Interior (−3.62% decade^{-1}) and Northeast Interior (−3.14% decade^{-1}), the evaluated negative MAM trend was not significant for Theil–Sen at the 90% confidence level, but both OLS regression and gamma regression returned significant model fits at 90% confidence, and gamma fits were superior [according to Akaike information criterion (AIC)] regression fits. Significant decreases in autumn (SON) SFE were evident in the West Coast (−4.31% decade^{-1}), Northwest Gulf (−3.62% decade^{-1}), North Panhandle (−3.24% decade^{-1}), and Aleutians (−6.87% decade^{-1}). In contrast, winter (DJF) trends were positive for all divisions except the Central Panhandle and South Panhandle, with significant increases in the West Coast (3.37% decade^{-1}), Cook Inlet (3.64% decade^{-1}), Bristol Bay (3.59% decade^{-1}), Northwest Gulf (3.15% decade^{-1}), and Northeast Gulf (2.53% decade^{-1}). The SFE trend in the Southeast Interior was positive, but only significant in the OLS and gamma regressions.

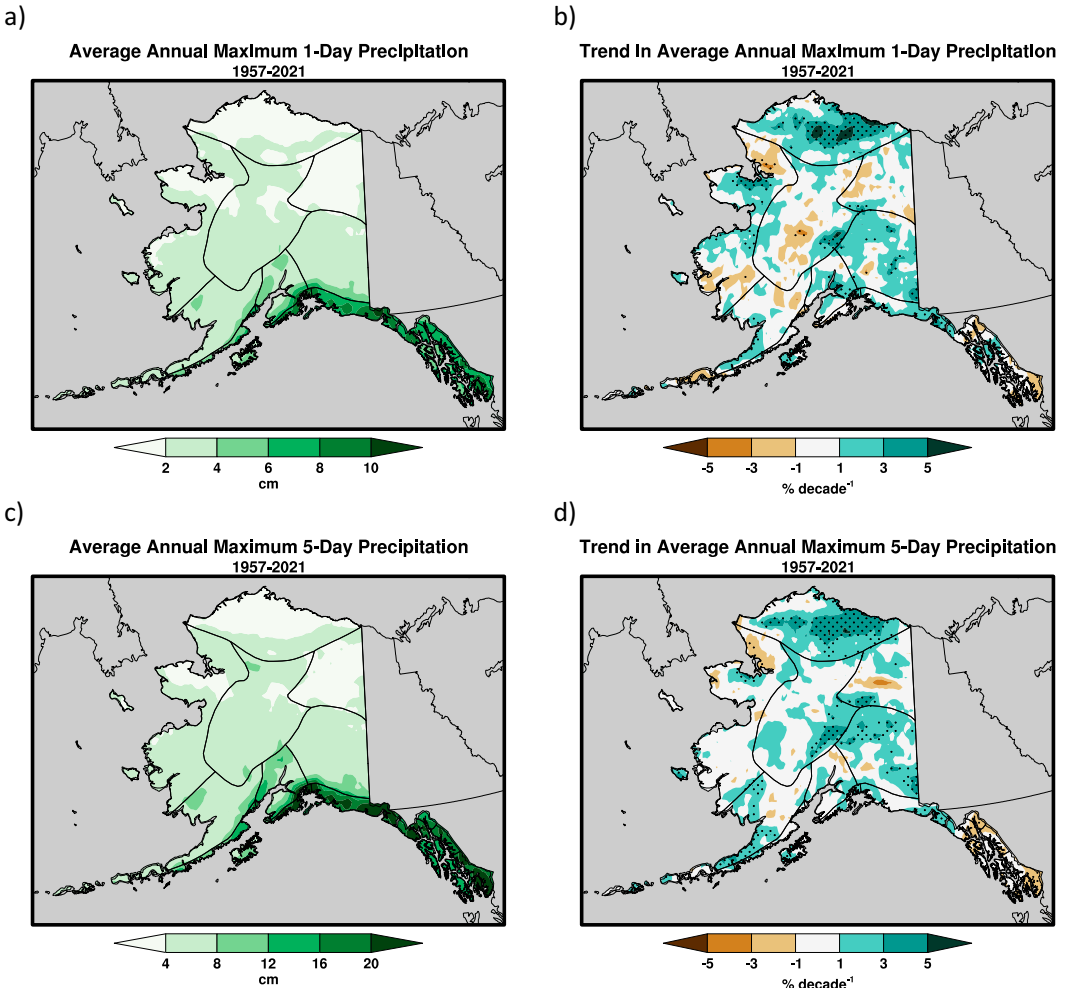

FIG. 8. (left) Mean values (cm) and (right) Theil–Sen trends (% decade^{-1}) of annual (a),(b) maximum 1-day precipitation and (c),(d) maximum 5-day precipitation. Significant trends, where $p \leq 0.10$, are stippled.

ONDJFMA and November–April (NDJFMA) SFE trends reflect this combination of negative and positive trends for different parts of the snow season and were rarely significant. ONDJFMA SFE decreased significantly in the South Panhandle (−2.80% decade^{-1}), and such trends were positive solely for the North Slope (1.75% decade^{-1}) and only for gamma regression. For NDJFMA, the North Slope (3.42% decade^{-1}) and Bristol Bay (2.50% decade^{-1}) trends were significant. The Central Interior had few significant trends, though a MAM decrease was significant for OLS and gamma regressions.

d. *Sea ice*

SIE surrounding Alaska has declined significantly over the passive microwave satellite record in the Bering, Chukchi, and Beaufort Seas (Fig. 9). The March SIE, the month of maximum coverage, decreased by ~50 000 km^2 decade^{-1} in the Bering Sea from 1957 to 2021. Over the past decade, the March SIE in the Bering Sea has exhibited markedly low coverage, with two record minimums in 2018 and 2019 (Perovich et al. 2019) that were associated with anomalously warm ocean temperatures (Thoman et al. 2020). For September, the month of minimum coverage, SIE declined by ~70 000 km^2 decade^{-1} in the Chukchi Sea and ~80 000 km^2 decade^{-1} in the Beaufort Sea from 1957 to 2021. Starting in the mid-1990s, the September sea ice loss accelerated in the Chukchi and Beaufort Seas. In the Bering Sea, September SIE is negligible. Sea ice reduction has a notable impact on terrestrial air temperatures over northern Alaska, as discussed in section 6.

The melt season has significantly lengthened in the Bering, Chukchi, and Beaufort Seas over 1979–2021 (Fig. 10). Based on Theil–Sen trends with 90% statistical significance, the date of continuous melt onset in the Bering Sea is occurring ~3.0 days decade^{-1} earlier, whereas continuous freeze onset is occurring ~3.0 days decade^{-1} later. The Chukchi Sea has a similar earlier trend in continuous melt onset (2.9 days decade^{-1}) but a larger delay in continuous freezing (5.0 days decade^{-1}) than in the Bering Sea. Changes in the Beaufort Sea's melt season are most striking of the three regions: continuous melt is occurring 6.0 days decade^{-1} earlier, while the date of continuous

TABLE 3. ERA5 mean values and Theil–Sen trends of annual RX1, maximum RX5 from 1957 to 2021. Significant trends that met the 90% confidence level are in bold.

Climate division	Code	RX1 mean (cm)	RX1 trend (% decade^{-1})	RX5 mean (cm)	RX5 trend (% decade^{-1})
North Slope	CD01	1.73	**2.34**	3.66	**2.17**
West Coast	CD02	2.21	0.20	4.81	−0.25
Central Interior	CD03	2.38	0.55	5.16	1.29
Northeast Interior	CD04	1.77	−0.35	3.64	0.55
Southeast Interior	CD05	2.81	**1.42**	6.05	**1.74**
Cook Inlet	CD06	4.45	1.32	10.35	0.74
Bristol Bay	CD07	3.27	0.27	7.14	0.60
Northwest Gulf	CD08	6.04	0.25	14.47	0.95
Northeast Gulf	CD09	7.81	1.00	19.36	0.76
North Panhandle	CD10	6.21	−0.83	15.76	−1.56
Central Panhandle	CD11	6.81	0.73	17.48	−1.03
South Panhandle	CD12	7.16	−1.22	17.69	−1.26
Aleutians	CD13	3.24	−0.69	6.76	0.34

freezing is 13.0 days decade^{-1} later, yielding a total lengthening of the melt season by 19.0 days decade^{-1} over 1979–2021.

6. Discussion

The trends obtained here for Alaska are occurring against a broader backdrop of Arctic change. In some cases, the trends align closely with larger-scale changes, while in other cases Alaska's terrestrial and marine climate are relatively anomalous. The broader-scale Arctic changes have been recently synthesized into a series of indicators by Box et al. (2019) and updated by Box et al. (2021). The Box et al. (2021) results for air temperature and precipitation are based primarily on the NCEP–NCAR reanalysis and generally for the 1971–2020 period, precluding precise alignment with the results reported here. However, general consistency is apparent in the key variables. For the Arctic land and ocean areas, Box et al. report positive temperature trends of 0.53° and 1.01°C decade^{-1} over 1971–2020. These values are larger than the 0.34°C decade^{-1} for Alaska over 1957–2021, but Box et al.'s Arctic land value is close to the statewide Alaska value of 0.45°C decade^{-1} for the 1971–2021 period (Table 1). As noted in section 5, however, the Alaska trend for the period beginning in 1971 is larger than the trend for earlier and later start years (1951, 1961, 1981, and 1991).

Box et al. (2021) report pan-Arctic precipitation trends of approximately 1.4% and 2.4% decade^{-1} for Arctic land and ocean areas, respectively. These changes are very similar to those obtained here for terrestrial Alaska over the 1957–2021 period, as shown in Fig. 6. Box et al. report a trend of −0.9% decade^{-1} in annual snowfall over Arctic land areas, again consistent with the findings of this study. However, Box et al.'s snowfall trend for the Arctic ocean areas is positive: +1.5% decade^{-1}, consistent with enhanced moisture availability from increasing areas of open water as sea ice retreats. The generally subfreezing air temperatures over the Arctic ocean areas favor a smaller increase of rain to snow ratios in comparison with Arctic land areas. Finally, Box et al. (2021) present data on recent changes in sea ice area over 1979–2020. The sea ice trends are based on the same passive microwave data sources used here for the 1979–2020 period, suggesting that quantitative differences relative to our results in section 5 could arise from our use of a longer time period for trend evaluation, the inclusion of presatellite observations, or other factors.

TABLE 4. Theil–Sen SFE trends (% decade^{-1}) by climate division for 1957–2021. Trends significant at 90% confidence are bolded. Significant trends at 90% confidence for OLS and/or gamma regression, but not Theil–Sen, are labeled with an asterisk.

Climate division	Code	September–August	DJF	MAM	SON	October–April	November–March
North Slope	CD01	0.12	2.85	0.97	0.30	1.75*	**3.42**
West Coast	CD02	−1.12	**3.37**	−3.32	**−4.31**	0.07	1.63
Central Interior	CD03	−0.69	2.70	−3.62*	−1.90	0.04	1.83
Northeast Interior	CD04	−0.82	2.90	−3.14*	−2.31	−0.03	2.26
Southeast Interior	CD05	−1.09	2.43*	**−3.32**	−1.11	−0.18	1.89
Cook Inlet	CD06	−0.26	**3.64**	**−3.72**	−1.84	0.98	1.91
Bristol Bay	CD07	−0.15	**3.59**	**−4.95**	−2.58	0.69	**2.50**
Northwest Gulf	CD08	−0.41	**3.15**	−2.88	**−3.62**	0.33	1.14
Northeast Gulf	CD09	−0.65	**2.53**	−2.48	−2.32	−0.21	0.96
North Panhandle	CD10	−1.55	1.46	−2.40	**−3.24**	−0.70	0.71
Central Panhandle	CD11	−2.01	−0.16	**−3.13**	−1.43	−1.15	−0.17
South Panhandle	CD12	**−3.29**	−2.22	−3.55	−2.88	**−2.80**	−1.80
Aleutians	CD13	−1.45	1.07	**−4.46**	**−6.87**	−0.71	0.51

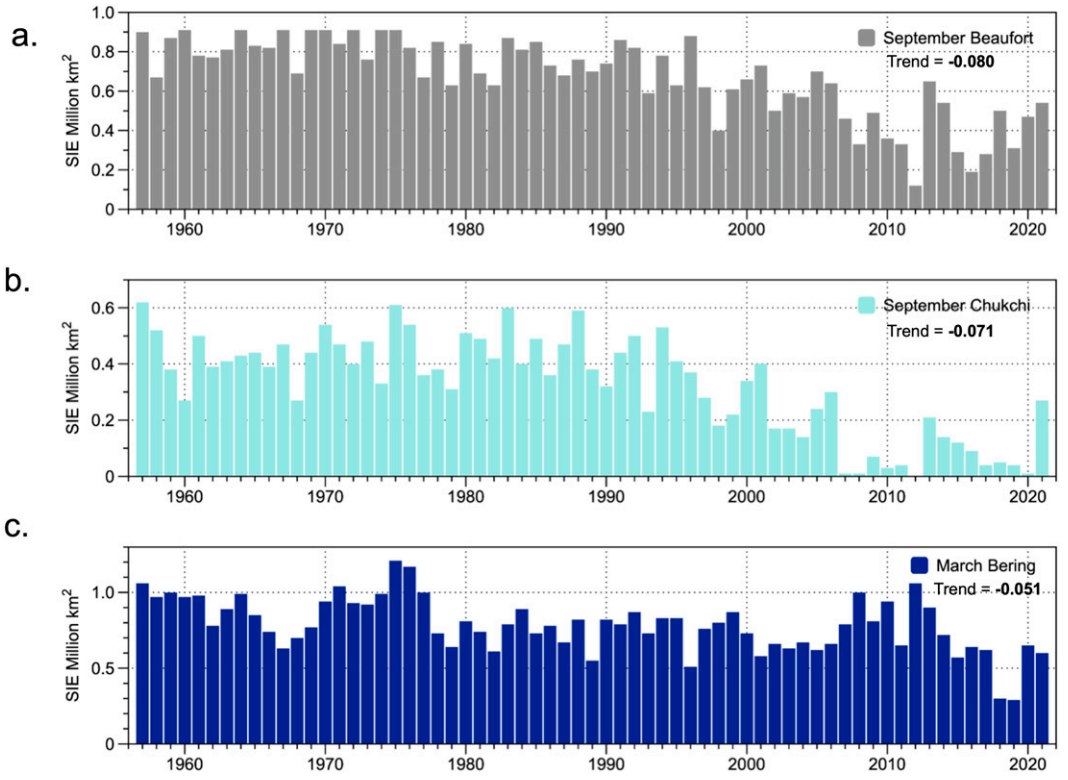

FIG. 9. Monthly SIE (million km^2) for (a) September Beaufort Sea, (b) September Chukchi Sea, and (c) March Bering Sea. Theil–Sen trends (million km^2 decade^{-1}) are shown in each panel. Significance is indicated in bold type at the 90% level or greater. The same colors associated with each marginal sea are carried over to Fig. 10.

Relationships among trends shown here are physically plausible. A striking example is the correspondence between sea ice loss (Fig. 9) and the increase of air temperature in northern Alaska, particularly in autumn (Wendler et al. 2014). Figure 4 shows that Alaska's North Slope, in closest proximity to the ice-diminished Beaufort and Chukchi Seas, has undergone substantially greater warming than the other Alaska climate divisions in all seasons except summer. However, the nature of the ice–temperature coupling is most apparent at coastal sites. Figure 11 shows the dramatic increase of October temperatures at Utqiaġvik, which is located on the Chukchi coast. The warming occurred rather abruptly in the early 2000s, when there was an acceleration of September sea ice loss in the Chukchi Sea (Fig. 9b). The increased areas of open water have allowed for increased solar heating of the upper ocean in summer, with a release of that heat to the atmosphere during autumn (Perovich and Richter-Menge 2009). In this respect, Utqiaġvik's October temperature history is a manifestation of the ice–albedo feedback, which is a key contributor to Arctic amplification. Figure 11 shows that this "climate shift" has been accompanied by a remarkable decrease in interannual variability, which is attributable to the moderating influence of the open water that is now widespread in October. While the 10 warmest Octobers in the 102-yr record are clustered in the most recent two decades, there has been a complete loss of monthly temperatures below the historical mean. Not only have none of the 10 coldest Octobers occurred in the past 20 years, the 20 most recent Octobers have fallen into the warmest tercile of the 102-yr distribution.

Precipitation and temperature provide a second example of interrelated trends. The recent increase of precipitation over Alaska is consistent with the increase of saturation vapor pressure associated with the warming atmosphere. This relationship is not unique to Alaska and is widely acknowledged as a factor in the increased intensity of heavy precipitation events worldwide (National Academies of Sciences, Engineering, and Medicine 2016). On the other hand, the increase of Alaska (and Arctic) precipitation has likely been further enhanced by the loss of sea ice and the increase of open water, as noted above. Climate modeling experiments have provided further support for the role of sea ice loss in the increase of Arctic precipitation (Higgins and Cassano 2009; Bintanja and Selten 2014). Conversely, the atmosphere is a driver of sea ice loss via warming over interannual to multidecadal time scales and by shifts in storm activity and their associated wind-forcing and thermal advection over shorter time scales (Cohen et al. 2020). Recent variations of sea ice in the Bering Sea provide striking examples of the importance of atmospheric forcing on subseasonal to seasonal time scales (Thoman et al. 2020).

The present study has focused on air temperature, precipitation, sea ice, and snowfall, which are key drivers of other parts of the Arctic system. As noted in section 1, Alaska contains

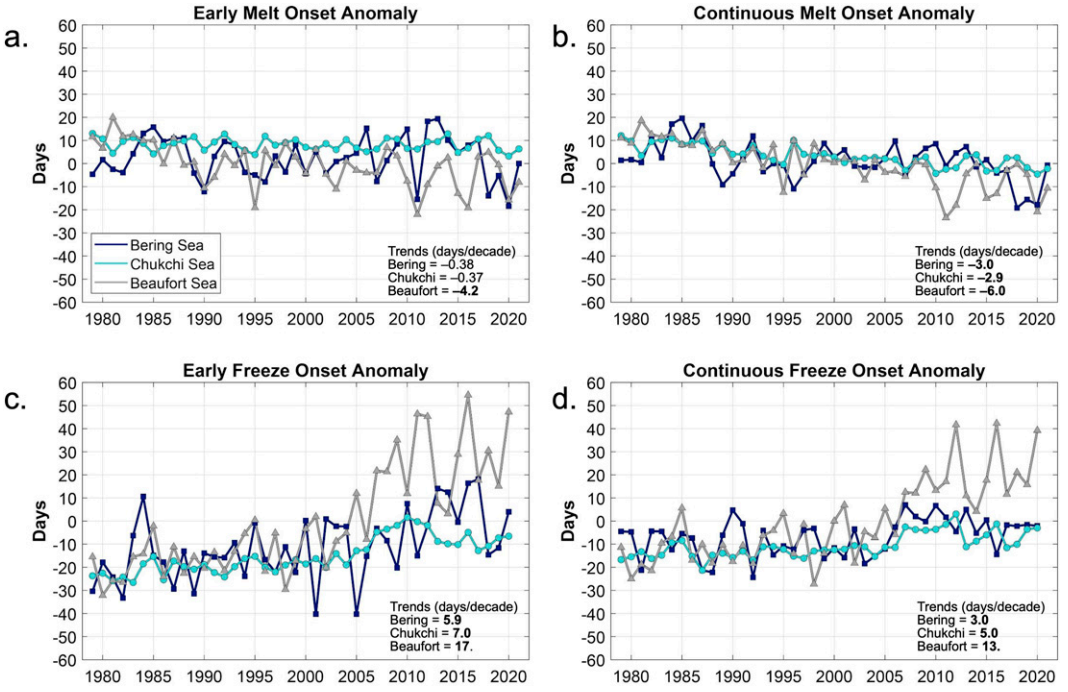

FIG. 10. Anomalies (relative to 1981–2010), in days, for the Bering, Chukchi, and Beaufort Seas for dates of (a) first melt onset (1979–2021), (b) continuous melt onset (1979–2021), (c) first freeze onset (1979–2020), and (d) continuous freeze onset (1979–2020). Theil–Sen melt season trends are shown in each panel with statistical significance, at the 90% level or greater, indicated by bold type. Statistically significant melt season duration trends (not shown) are 6.0, 7.9, and 19.0 days decade^{-1} for the Bering, Chukchi, and Beaufort Seas, respectively.

extensive areas of permafrost and numerous glaciers. Both of these cryospheric variables are responding to a warmer climate (Arctic Monitoring and Assessment Programme 2017, 2021), although changes in snowfall can complicate the thermal response of glaciers as well as permafrost. Warming temperatures are also associated with summer drying unless the increased evapotranspiration is offset by an increase of precipitation. The recent increase in the frequency of severe wildfire years in Alaska suggests that the increased evapotranspiration is not being offset by increased precipitation (Partain et al. 2016; Bhatt et al. 2021). However, changes in vegetation in Alaska are also consistent with increased temperature and precipitation (Rees et al. 2020; Parker et al. 2021). These various changes are almost certainly impacting terrestrial and marine ecosystems in the Alaska region, although such impacts are beyond the scope of this paper.

Finally, Alaska's warming of the past 70 years can be compared to the warming over the same period in other parts of the United States, including the entire contiguous United States and its various climatic regions. Table 5 provides such a comparison with NCEI ACD data. Subject to the constraint of the choice of 1957–2021 as the reference period, Table 5 shows that Alaska's rate of warming during this period exceeded the rate for the contiguous United States by more than 50%. Alaska's rate of warming (0.34°C decade^{-1}) was also greater than that of any of the U.S. climate regions, for which the rates ranged from 0.17°C decade^{-1} in the Northwest region to 0.27°C decade^{-1} in the Northeast region. In this respect, Alaska is indeed at the forefront of climate warming in the United States.

7. Conclusions

The main conclusions of our study on Alaska climate trends are summarized below by the four main parameters that were examined, with an emphasis (except for sea ice characteristics) on ERA5 results for the full 1957–2021 period.

- *Temperature*: Annual T2m trends are positive and statistically significant ($p \leq 0.10$) across all climate divisions, with the largest Theil–Sen trends found on the North Slope and North Panhandle division (>0.50°C decade^{-1}). Similarly, at the seasonal scale these divisions showed the largest trends in winter, spring, or autumn with the North Slope (≥0.69°C decade^{-1} in spring and autumn) and North Panhandle (≥0.78°C decade^{-1} in winter and spring) changes being nearly ~3.5°C over the analysis period. Extreme temperature trends (i.e., 99th percentile) were largely positive but significant mainly in southern and western mainland Alaska.
- *Precipitation*: While spatially heterogeneous, all climate divisions showed positive annual total precipitation trends but were only significant for the North Slope and Southeast Interior. At the seasonal scale, winter and summer saw the most divisions with significant trends, but only the Northeast Gulf had a significant trend in both seasons (winter, 3.70% decade^{-1}; summer, 5.32% decade^{-1}). The aforementioned

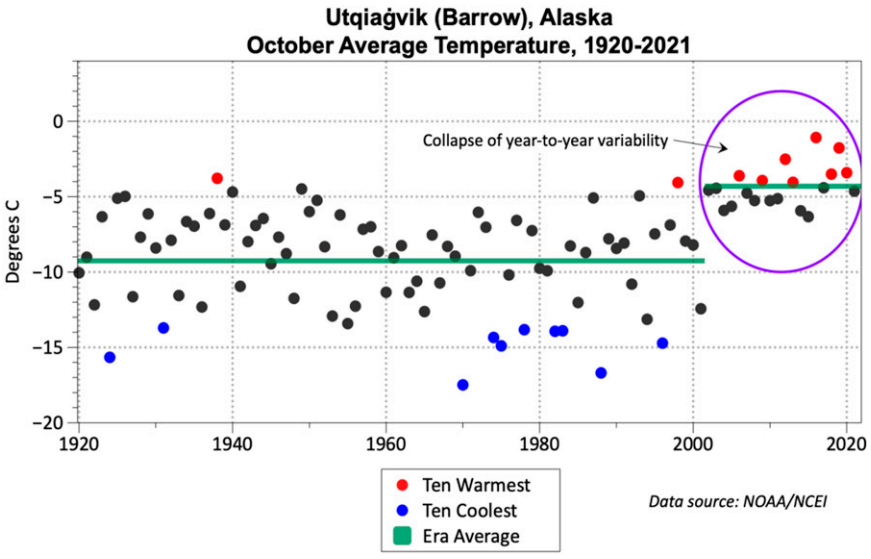

FIG. 11. Average temperature at Utqiaġvik, Alaska, for each October from 1920 to 2021. Red and blue dots denote the 10 warmest and coldest Octobers, respectively. Horizontal green lines show subperiod means for 1920–2001 and 2002–21.

North Slope and Southeast Interior divisions also saw the only significant 1- and 5-day precipitation trends. At the North Slope, the change in precipitation and extremes suggests an accelerating hydrological response to Arctic warming is ongoing.

- *Snowfall*: Several of the southerly divisions (e.g., Bristol Bay, Northwest Gulf, South Panhandle, the Aleutians) have significant negative trends for multiple seasons, including spring and autumn, with Bristol Bay and the Aleutians having strong evidence for changes in all seasons. Winter SFE is generally increasing across divisions, but spring and autumn have a wider expression of SFE decreases, showing clear erosion of the snowfall season further north (e.g., North Slope, West Coast, Northeast Interior) in addition to the more southerly divisions.
- *Sea ice*: During March, the month of maximum Arctic ice coverage, Bering SIE has declined by ~50 000 km^2 decade^{-1} since 1957. During the September minimum, Beaufort and Chukchi SIE has declined by 80 000 and 70 000 km^2 decade^{-1}, respectively. In addition to the Beaufort Sea's striking SIE reduction, melt onset is earlier (6.05 days decade^{-1}), and the date of continuous freeze is much later (12.76 days decade^{-1}), yielding a total lengthening of the melt season by almost three weeks since 1979. Compared to the initial study of Markus et al. (2009), our results suggest an approximate Beaufort and Chukchi melt season lengthening of nearly one week in the last decade alone.

TABLE 5. Comparison of NCEI ACD Alaska statewide temperature OLS and Theil–Sen trends with trends over NOAA NCEI U.S. Climate Regions during 1957–2021.

Region	OLS trend (°C decade^{-1})	Theil–Sen trend (°C decade^{-1})
Alaska	0.34	0.35
Contiguous United States	0.22	0.22
Ohio Valley	0.22	0.23
Upper Midwest	0.24	0.25
Northeast	0.27	0.26
Northwest	0.17	0.17
South	0.21	0.20
Southeast	0.24	0.24
Southwest	0.25	0.26

Future work will further compare and expand upon Alaska trends versus those of Arctic terrestrial subregions using ERA5 reanalysis and, in the case of snow and sea ice, leverage new satellite products (e.g., *Sentinel-3* and *ICESat-2*). Such rate-of-change analyses and the creation of benchmarks in new parameters (i.e., snow depth on land and sea ice thickness) will be informative for future climate assessments and annual reports (e.g., NOAA Arctic Report Card and *Bulletin of the American Meteorological Society* special section State of the Climate), while continuing to place Alaska climate change in context of other Arctic rapid-change regions. Further work is also needed to quantify the linkages between trends of the variables described in this paper and ecosystem changes in Alaska and its coastal seas.

Acknowledgments. We appreciate constructive comments from Editor Shawn Marshall, Pamela Sousanes (USNPS), and three anonymous reviewers that led to manuscript improvements at revision stage. Special thanks to Julien Nicolas and Hans Hersbach for providing details on Alaska's weather stations assimilated into ERA5. Alaska climate division ERA5 trends were calculated in R V4.1.1 (R Core Team 2022) and NCL V6.6.2 (NCAR 2019). M.A.W. conducted this work under NASA's Weather and Atmospheric Dynamics program

(80NSSC20K0922). T.J.B., U.S.B., R.T.L., P.A.B., and C.F.W. were supported by Alaska EPSCoR NSF Award OIA-1757348, and the state of Alaska. U.S.B. and P.A.B. were also supported by Grant G17AC00363 and the Alaska Climate Adaptation Science Center (AKCASC) through Cooperative Agreement G10AC00588 from the U.S. Geological Survey (USGS). This paper's contents are solely the responsibility of the authors, supported by the USGS, and do not necessarily represent the views of AKCASC. All authors contributed equally to this work. The authors do not declare any conflicts of interest. Any use of trade, firm, or product names is for descriptive purposes only and does not imply endorsement by the U.S. government.

Data availability statement. All data are available via open archives. ERA5 data are obtained from Copernicus (https://cds.climate.copernicus.eu/cdsapp#!/dataset/reanalysis-era5-pressure-levels?tab=overview). NOAA NClimGrid data are accessed from https://www.ncei.noaa.gov/access/metadata/landing-page/bin/iso?id=gov.noaa.ncdc:C00332. NOAA NCEI ACD data are obtained from https://www.ncdc.noaa.gov/cag/. Gridded passive microwave sea ice concentration and the sea ice index are available from NSIDC (https://masie_web.apps.nsidc.org/pub//DATASETS/NOAA/G02135/). Sea ice melt and freeze onsets products are available at https://earth.gsfc.nasa.gov/cryo/data/arctic-sea-ice-melt.

REFERENCES

Arctic Monitoring and Assessment Programme, 2005: *Arctic Climate Impact Assessment*. Cambridge University Press, 1042 pp.

——, 2017: *Snow, Water, Ice and Permafrost in the Arctic (SWIPA) 2017*. AMAP, 269 pp.

——, 2021: *Arctic Climate Change Update 2021: Key Trends and Impacts*. AMAP, 148 pp.

Arguez, A., I. Durre, S. Applequist, R. S. Vose, M. F. Squires, X. Yin, R. R. Heim Jr., and T. W. Owen, 2012: NOAA's 1981–2010 U.S. Climate Normals: An overview. *Bull. Amer. Meteor. Soc.*, **93**, 1687–1697, https://doi.org/10.1175/BAMS-D-11-00197.1.

Avila-Diaz, A., D. H. Bromwich, A. B. Wilson, F. Justino, and S.-H. Wang, 2021: Climate extremes across the North American Arctic in modern reanalyses. *J. Climate*, **34**, 2385–2410, https://doi.org/10.1175/JCLI-D-20-0093.1.

Bachand, C. L., and J. E. Walsh, 2022: Extreme precipitation events in Alaska: Historical trends and projected changes. *Atmosphere*, **13**, 388, https://doi.org/10.3390/atmos13030388.

Ballinger, T. J., and J. E. Overland, 2022: The Alaskan Arctic regime shift since 2017: A harbinger of years to come? *Polar Sci.*, **32**, 100841, https://doi.org/10.1016/j.polar.2022.100841.

Barrett, A. P., J. C. Stroeve, and M. C. Serreze, 2020: Arctic Ocean precipitation from atmospheric reanalyses and comparisons with North Pole drifting station records. *J. Geophys. Res. Oceans*, **125**, e2019JC015415, https://doi.org/10.1029/2019JC015415.

Bhatt, U. S., and Coauthors, 2021: Climate drivers of Arctic tundra variability and change using an indicators framework. *Environ. Res. Lett.*, **16**, 055019, https://doi.org/10.1088/1748-9326/abe676.

Bieniek, P. A., and J. E. Walsh, 2017: Atmospheric circulation patterns associated with monthly and daily temperature and precipitation extremes in Alaska. *Int. J. Climatol.*, **37**, 208–217, https://doi.org/10.1002/joc.4994.

——, and Coauthors, 2012: Climate divisions for Alaska based on objective methods. *J. Appl. Meteor. Climatol.*, **51**, 1276–1289, https://doi.org/10.1175/JAMC-D-11-0168.1.

——, J. E. Walsh, R. L. Thoman, and U. S. Bhatt, 2014: Using climate divisions to analyze variations and trends in Alaska temperature and precipitation. *J. Climate*, **27**, 2800–2818, https://doi.org/10.1175/JCLI-D-13-00342.1.

Bigalke, S., and J. E. Walsh, 2022: Future changes of snow in Alaska and the Arctic under stabilized global warming scenarios. *Atmosphere*, **13**, 541, https://doi.org/10.3390/atmos13040541.

Bintanja, R., and F. M. Selten, 2014: Future increases in Arctic precipitation linked to local evaporation and sea-ice retreat. *Nature*, **509**, 479–482, https://doi.org/10.1038/nature13259.

Box, J. E., and Coauthors, 2019: Key indicators of Arctic climate change: 1971–2017. *Environ. Res. Lett.*, **14**, 045010, https://doi.org/10.1088/1748-9326/aafc1b.

——, and Coauthors, 2021: Recent developments in Arctic climate observational indicators. *AMAP Arctic Climate Change Update 2021: Key Trends and Impacts*, J. E. Box et al., Eds., Arctic Monitoring and Assessment Programme, 7–29.

Cabaj, A., P. J. Kushner, C. G. Fletcher, S. Howell, and A. A. Petty, 2020: Constraining reanalysis snowfall over the Arctic Ocean using CloudSat observations. *Geophys. Res. Lett.*, **47**, e2019GL086426, https://doi.org/10.1029/2019GL086426.

Cohen, J., and Coauthors, 2020: Divergent consensus on Arctic amplification influence on midlatitude severe winter weather. *Nat. Climate Change*, **10**, 20–29, https://doi.org/10.1038/s41558-019-0662-y.

Dou, T., and Coauthors, 2021: Trends and spatial variation in rain-on-snow events over the Arctic Ocean during the early melt season. *Cryosphere*, **15**, 883–895, https://doi.org/10.5194/tc-15-883-2021.

Earth Resources Observation and Science Center/U.S. Geological Survey/U.S. Department of the Interior, 1997: USGS 30 arc-second Global Elevation Data, GTOPO30. NCAR Research Data Archive, https://doi.org/10.5065/A1Z4-EE71.

Farr, T. G., and Coauthors, 2007: The Shuttle Radar Topography Mission. *Rev. Geophys.*, **45**, RG2004, https://doi.org/10.1029/2005RG000183.

Fetterer, F., K. Knowles, W. N. Meier, M. Savoie, and A. K. Windnagel, 2017: Updated daily: Sea Ice Index, version 3. National Snow and Ice Data Center, accessed 15 April 2022, https://doi.org/10.7265/N5K072F8.

Frey, K. E., G. W. K. Moore, L. W. Cooper, and J. M. Grebmeier, 2015: Divergent patterns of recent sea ice cover across the Bering, Chukchi, and Beaufort Seas of the Pacific Arctic region. *Prog. Oceanogr.*, **136**, 32–49, https://doi.org/10.1016/j.pocean.2015.05.009.

Fyfe, J. C., K. von Salzen, N. P. Gillett, V. K. Arora, G. M. Flato, and J. R. McConnell, 2013: One hundred years of Arctic surface temperature variations due to anthropogenic influence. *Sci. Rep.*, **3**, 2645, https://doi.org/10.1038/srep02645.

Graham, R. M., S. R. Hudson, and M. Matarilli, 2019: Improved performance of ERA5 in Arctic gateway relative to four global atmospheric reanalyses. *Geophys. Res. Lett.*, **46**, 6138–6147, https://doi.org/10.1029/2019GL082781.

Grant, A. N., S. Brönnimann, T. Ewen, and A. Nagurny, 2009: A new look at radiosonde data prior to 1958. *J. Climate*, **22**, 3232–3247, https://doi.org/10.1175/2008JCLI2539.1.

Hartmann, B., and G. Wendler, 2005: The significance of the 1976 Pacific climate shift in the climatology of Alaska. *J. Climate*, **18**, 4824–4839, https://doi.org/10.1175/JCLI3532.1.

Hersbach, H., and Coauthors, 2020: The ERA5 global reanalysis. *Quart. J. Roy. Meteor. Soc.*, **146**, 1999–2049, https://doi.org/10.1002/qj.3803.

Higgins, M. E., and J. J. Cassano, 2009: Impacts of reduced sea ice on winter Arctic atmospheric circulation, precipitation, and temperature. *J. Geophys. Res.*, **114**, D16107, https://doi.org/10.1029/2009JD011884.

IPCC, 2001: *Climate Change 2001: Synthesis Report*. Cambridge University Press, 398 pp.

Lader, R., J. E. Walsh, U. S. Bhatt, and P. A. Bieniek, 2017: Projections of 21st century climate extremes for Alaska via dynamical downscaling and quantile mapping. *J. Appl. Meteor. Climatol.*, **56**, 2393–2409, https://doi.org/10.1175/JAMC-D-16-0415.1.

Lindsay, C., J. Zhu, A. E. Miller, P. Kirchner, and T. L. Wilson, 2015: Deriving snow cover metrics for Alaska from MODIS. *Remote Sens.*, **7**, 12 961–12 985, https://doi.org/10.3390/rs71012961.

López-de-Lacalle, J., 2012: Trends in Alaska temperature data. Towards a more realistic approach. *Climate Dyn.*, **38**, 2131–2141, https://doi.org/10.1007/s00382-011-1198-7.

Markon, C., and Coauthors, 2018: Alaska. *Impacts, Risks, and Adaptation in the United States: Fourth National Climate Assessment*, D. R. Reidmiller et al., Eds., Vol. II, U.S. Global Change Research Program, 1185–1241, https://doi.org/10.7930/NCA4.2018.CH26.

Markus, T., J. C. Stroeve, and J. Miller, 2009: Recent changes in Arctic sea ice melt onset, freeze-up, and melt season length. *J. Geophys. Res.*, **114**, C12024, https://doi.org/10.1029/2009JC005436.

McAfee, S. A., G. S. Guentchev, and J. K. Eischeid, 2013: Reconciling precipitation trends in Alaska: 1. Station-based analyses. *J. Geophys. Res. Atmos.*, **118**, 7523–7541, https://doi.org/10.1002/jgrd.50572.

McAfee, S., G. Guentchev, and J. Eischeid, 2014: Reconciling precipitation trends in Alaska: 2. Gridded data analyses. *J. Geophys. Res. Atmos.*, **119**, 13 820–13 837, https://doi.org/10.1002/2014JD022461.

McCrystall, M. R., J. Stroeve, M. Serreze, B. C. Forbes, and J. A. Screen, 2021: New climate models reveal faster and larger increases in Arctic precipitation than previously projected. *Nat. Commun.*, **12**, 6765, https://doi.org/10.1038/s41467-021-27031-y.

Meier, W. N., J. S. Stewart, A. Windnagel, and F. M. Fetterer, 2022: Comparison of hemispheric and regional sea ice extent and area trends from NOAA and NASA passive microwave-derived climate records. *Remote Sens.*, **14**, 619, https://doi.org/10.3390/rs14030619.

Mizukami, N., and Coauthors, 2022: New projections of 21st century climate and hydrology for Alaska and Hawai'i. *Climate Serv.*, **27**, 100312, https://doi.org/10.1016/j.cliser.2022.100312.

Moon, T. A., M. L. Druckenmiller, and R. L. Thoman, 2021: Arctic Report Card 2021: Executive summary. NOAA Tech. Rep. OAR ARC 21-01, 4 pp., https://doi.org/10.25923/5s0f-5163.

National Academies of Sciences, Engineering, and Medicine, 2016: *Attribution of Extreme Weather Events in the Context of Climate Change*. National Academies Press, 165 pp., https://doi.org/10.17226/21852.

NCAR, 2019: The NCAR Command Language. UCAR/NCAR/CISL/TDD, https://doi.org/10.5065/D6WD3XH5.

Nelder, J. A., and R. W. M. Wedderburn, 1972: Generalized linear models. *J. Roy. Stat. Soc.*, **135A**, 370–384, https://doi.org/10.2307/2344614.

Parker, T. C., A. M. Thurston, K. Raundrup, J.-A. Subke, P. A. Wookey, and I. P. Hartley, 2021: Shrub expansion in the Arctic may induce large-scale carbon losses due to changes in plant-soil interactions. *Plant Soil*, **463**, 643–651, https://doi.org/10.1007/s11104-021-04919-8.

Partain, J. L., Jr., and Coauthors, 2016: An assessment of the role of anthropogenic climate change in the Alaska fire season of 2015 [in "Explaining Extremes of 2015 from a Climate Perspective"]. *Bull. Amer. Meteor. Soc.*, **97** (12), S14–S18, https://doi.org/10.1175/BAMS-D-16-0149.1.

Perovich, D., and J. A. Richter-Menge, 2009: Loss of sea ice in the Arctic. *Annu. Rev. Mar. Sci.*, **1**, 417–441, https://doi.org/10.1146/annurev.marine.010908.163805.

——, and Coauthors, 2019: Sea ice. *NOAA Arctic Report Card 2019*, J. Richter-Menge et al., Eds., NOAA, 26–34, https://arctic.noaa.gov/Report-Card/Report-Card-2019/ArtMID/7916/ArticleID/841/Sea-Ice.

Pettitt, A. N., 1979: A non-parametric approach to the change-point problem. *J. Roy. Stat. Soc.*, **28C**, 126–135, https://doi.org/10.2307/2346729.

Pohlert, T., 2020: trend: Non-parametric trend tests and change-point detection, version 1.1.4. R package, https://CRAN.R-project.org/package=trend.

Räisänen, J., 2021: Effect of atmospheric circulation on surface air temperature trends in years 1979–2018. *Climate Dyn.*, **56**, 2303–2320, https://doi.org/10.1007/s00382-020-05590-y.

R Core Team, 2022: R: A language and environment for statistical computing. R Foundation for Statistical Computing, https://www.R-project.org/.

Rees, G., and Coauthors, 2020: Is subarctic forest advance able to keep pace with climate change? *Global Change Biol.*, **26**, 3965–3977, https://doi.org/10.1111/gcb.15113.

Rolph, R. J., A. R. Mahoney, J. Walsh, and P. A. Loring, 2018: Impacts of a lengthening open water season on Alaskan coastal communities: Deriving locally relevant indices from large-scale datasets and community observations. *Cryosphere*, **12**, 1779–1790, https://doi.org/10.5194/tc-12-1779-2018.

Sen, P. K., 1968: Estimates of regression coefficient based on Kendall's tau. *J. Amer. Stat. Assoc.*, **63**, 1379–1389, https://doi.org/10.1080/01621459.1968.10480934.

Swanson, D. K., 2017: Trends in greenness and snow cover in Alaska's Arctic national parks, 2000–2016. *Remote Sens.*, **9**, 514, https://doi.org/10.3390/rs9060514.

Theil, H., 1950: A rank invariant method of linear and polynomial regression analysis, 2-3; confidence regions for the parameters of linear regression equations in two, three, and variables. *Proc. Nederl. Akad. Wetensch.*, **53**, 386–392.

Thoman, R., and J. E. Walsh, 2019: Alaska's changing environment: Documenting Alaska's physical and biological changes through observations. International Arctic Research Center, 16 pp., https://uaf-iarc.org/wp-content/uploads/2019/08/Alaskas-Changing-Environment_2019_WEB.pdf.

——, and Coauthors, 2020: The record low Bering Sea ice extent in 2018: Context, impacts, and an assessment of the role of anthropogenic climate change [in "Explaining Extremes of 2018 from a Climate Perspective"]. *Bull. Amer. Meteor. Soc.*, **101** (1), S53–S57, https://doi.org/10.1175/BAMS-D-19-0175.1.

Vose, R. S., and Coauthors, 2014: Improved historical temperature and precipitation time series for US climate divisions. *J. Appl. Meteor. Climatol.*, **53**, 1232–1251, https://doi.org/10.1175/JAMC-D-13-0248.1.

——, and Coauthors, 2017: Deriving historical temperature and precipitation time series for Alaska climate divisions via

climatologically aided interpolation. *J. Serv. Climatol.*, https://doi.org/10.46275/JoASC.2017.10.001.

Walsh, J. E., and B. Brettschneider, 2019: Attribution of recent warming in Alaska. *Polar Sci.*, **21**, 101–109, https://doi.org/10.1016/j.polar.2018.09.002.

——, F. Fetterer, J. S. Stewart, and W. L. Chapman, 2017: A database for depicting Arctic sea ice variations back to 1850. *Geogr. Rev.*, **107**, 89–107, https://doi.org/10.1111/j.1931-0846.2016.12195.x.

——, D. H. Bromwich, J. E. Overland, M. C. Serreze, and K. R. Wood, 2018: 100 years of progress in polar meteorology. *A Century of Progress in Atmospheric and Related Sciences: Celebrating the American Meteorological Society Centennial*, *Meteor. Monogr.*, No. 59, Amer. Meteor. Soc., https://doi.org/10.1175/AMSMONOGRAPHS-D-18-0003.1.

Wang, C., R. M. Graham, K. Wang, S. Gerland, and M. A. Granskog, 2019: Comparison of ERA5 and ERA-Interim near-surface air temperature, snowfall and precipitation over Arctic sea ice effects on sea ice thermodynamics and evolution. *Cryosphere*, **13**, 1661–1679, https://doi.org/10.5194/tc-13-1661-2019.

Wendler, G., B. Moore, and K. Galloway, 2014: Strong temperature increase and shrinking sea ice in Arctic Alaska. *Open Atmos. Sci. J.*, **8**, 7–15, https://doi.org/10.2174/1874282301408010007.

White, J. H. R., J. E. Walsh, and R. L. Thoman Jr., 2021: Using Bayesian statistics to detect trends in Alaskan precipitation. *Int. J. Climatol.*, **41**, 2045–2059, https://doi.org/10.1002/joc.6946.

Yang, D., D. Kane, and Z. Zhang, 2005: Bias correction of long-term (1973–2014) daily precipitation data over the northern regions. *Geophys. Res. Lett.*, **32**, L19501, https://doi.org/10.1029/2005GL024057.